Hindawi
Mathematical Problems in Engineering
Volume 2020, Article ID 6725408, 11 pages
https://doi.org/10.1155/2020/6725408

Research Article

Research of Vehicle Rear-End Collision Model considering Multiple Factors

Qiang Luo,[1] Xiaodong Zang,[1] Jie Yuan,[1] Xinqiang Chen,[2] Junheng Yang,[1] and Shubo Wu[3]

[1]*School of Civil Engineering, Guangzhou University, Guangzhou, China*
[2]*Institute of Logistics Science and Engineering, Shanghai Maritime University, Shanghai, China*
[3]*Merchant Marine College, Shanghai Maritime University, Shanghai, China*

Correspondence should be addressed to Jie Yuan; yuanj@gzhu.edu.cn and Xinqiang Chen; chenxinqiang@stu.shmtu.edu.cn

Received 25 September 2019; Revised 10 January 2020; Accepted 19 March 2020; Published 10 April 2020

Academic Editor: Chen-Feng Li

The accuracy of the rear-end collision models is crucial for the early warning of potential traffic accident identification, and thus analyzes of the main factors influencing the rear-end collision relevant models is an active topic in the field. The previous studies have tried to determine the single factor influence on the rear-end collision model performance. Less attention was paid to exploit mutual influences on the model performance. To bridge the gap, we proposed an improved vehicle rear-end collision model by integrating varied factors which influence two parameters (i.e., response time and road adhesion coefficient). The two parameters were solved with the integrated weighting and neural network models, respectively. After that we analyzed the relationship between varied factors and the minimum car-following distance. The research findings support both the theoretical and practical guidance for transportation regulations to release more reasonable minimum headway distance to enhance the roadway traffic safety.

1. Introduction

A large number of traffic accident investigations indicate that the vehicle rear-end accident takes up a relatively high proportion and is one of the main forms of traffic accidents. If an accurate rear-end collision avoidance system can be established, it will be able to remind the driver to maintain a safe following distance in time and effectively avoid rear-end collisions. The vehicle rear-end collision avoidance model is mainly used to study the car-following relationship between the leading and following vehicles and provide the safety distance to be maintained to the following vehicle. The safe distance should be sufficient for the following vehicle' driver who has sufficient reaction time to slow down when the leading vehicle conducts emergency brake for preventing rear-end collision. Some studies have found that the safety of car following and the required safety following distance are affected by many factors, such as driver characteristics, weather, and road conditions [1–4].

On the basis of the traditional safety distance model, Kong et al. conducted information acquisition, distance judgment, braking, and other processes for active collision avoidance during vehicle travel. However, the judgment model used is relatively simple [5]. Jiang and Yu established a highway antitailing model based on radial basis function neural network by using traditional algorithms [6]. Nevertheless, the model is mainly applied to highways, and the influencing factors are considered to be single. Jing and Wang explored the influence of multiple vehicles on the driver and established a vehicle-following model considering the traffic state based on the full velocity difference (FVD) model [7]. Nonetheless, the model is too complicated to conduct to practical applications. Xia established a fuzzy inference system based on the characteristics (e.g., driving age, and gender) of the driver to determine the response time of different drivers and proposed an improved version of the safe model [8]. Peng and Sun derived the modified Korteweg–de Vries (mKdV) equation to describe the traffic

behavior near the critical point by using linear stability theory and proposed an improved car-following (MCF) model based on the full velocity difference (FVD) model and considering multiple information inputs from preceding vehicles [9]. Wilson and Ward suggested that all vehicle car-following models should be tested for stability to ensure improved performance [10]. Tan and Huang [11] proposed a cooperative collision warning system for vehicle-to-vehicle based on DGPS. However, the safety distance algorithm does not consider the driver's driving characteristics and actual road conditions; thus, the practical application of the warning system is low. Huang et al. [12] trained the car-following model by using the LSTM (long short-term memory) neural network, but the network belongs to a deep neural network with multiple hidden layers. The structure of the network has too much target parameters and is complex.

Previous studies suggested that the safe following distance is mainly affected by drivers' characteristics, the acceleration/deceleration performance of vehicles, weather situations, and road conditions [1–3, 8, 9]. It is noted that less attention was paid to analyze the intrinsic relations between the abovementioned typical factors and the minimum car-following models. To address the issue, we systematically analyzed main factors influencing car-following distance from the perspective of driver-vehicle-road-environment and quantified the main factors' influences with two parameters (i.e., reaction time and pavement adhesion coefficient) because the main influencing factors on traffic safety come from these four aspects in the road transportation system. Then, we have considered the driver (age, fatigue level, and driving style), vehicle (vehicle grade, service life ratio, and accident record), weather, and road factors (whether the road segment is normal, new/old, and road width) to evaluate the response time correction factor. In addition, we studied the road conditions, tire pressure, and vehicle speed for quantifying the pavement adhesion coefficient influence. We employed the integrated weighting model to obtain the maximum value for the response time correction factor, and the neural network was introduced to obtain the optimal value for the pavement adhesion coefficient parameter. Based on that we established a vehicle rear-end collision model, which was further testified on different traffic scenarios.

2. Analysis of Influencing Factors

Previous studies suggested that the four factors (i.e., driver, vehicle, road, and environment) are considered as the main factors for estimating the minimal safety distance in the vehicle rear-end collision models [4, 12–15]. We followed the same rule when establishing our vehicle rear-end collision model.

2.1. Driver Factors. Driver factors are divided into two aspects: the physiological and psychological factors. The physiological factors are mainly reflected in the driver's age and fatigue level, and the psychological factors are mainly reflected in the driver's driving style [15–17]. Brocn and Chiang collected the reaction time of 100 drivers, and the results showed that the response time increases as the age increases [18]. Yu got drivers' reaction time under both the normal sate and the fatigue state (as shown in Table 1). Obviously, the reaction time of the driver in the fatigue state is greater than that in the normal state. The reaction time at different ages varies, and the greatest difference in response time was in the age group 22–45 [19]. Zhang et al. divided driving behavior types into five categories: conservative, cautious, conventional, radical, and adventurous [20]. The reaction time of five types of drivers was tested on two different braking modes of vehicles (i.e., hydraulic braking or pneumatic braking). The result shows that the driver with a conservative driving style has the longest reaction time regardless of the braking method of the vehicle. The reaction time of the radical driver is minimum for the hydraulic brake vehicle and that of the adventurous driver is minimum for the pneumatic brake vehicle.

Our previous studies suggested that the driver reaction time is significantly positively relevant with driver fatigue magnitude, which can be quantified into the interval of [0, 10] [19]. More specifically, we consider that the driver fatigue degree is considered as a continuous parameter demonstrating the driver's travelling time on roadway.

2.2. Vehicle Factors. A wide variety of vehicles, including cars and large trucks, are available, and high- and low-end cars exist in the same model. The power performance and breaking style of various types and grades of vehicles differ and determine the maximum speed and maximum brake deceleration. In addition, the service life and accident rate of the vehicle will affect the vehicle performance, which affects driving safety in turn [20].

2.3. Weather Factors. The driving environment also has an impact on the drivers' reaction time. In sunny weather with a good view, driving is safe and the response time required to perform various driving operations is short. By contrast, driving is dangerous and the response time required to perform various driving operations is long in bad weather with poor view [21]. In addition, in bad weather, such as when it is raining, it is prone to slipping and braking errors, and the friction coefficient of the road surface will be reduced.

2.4. Road Factors. The impact of road factors on car-following safety is mainly derived from the friction coefficient between the vehicle and the road surface, that is, the adhesion coefficient, which affects the braking effect of vehicle. When the adhesion coefficient is large, the adhesion is large and the driving safety is high. The size of the adhesion coefficient mainly depends on the condition of the road surface and the tire, and the road surface factors mainly include the type of road surface, roughness and dryness, and humidity. The tire factor is mainly the tread pattern of the tire, that is, the type and depth of the tread [22–24].

Table 1: Reaction time of the driver under both the normal sate and the fatigue state.

Age group	Normal state (s)	Fatigue state (s)
18~22	0.48~0.56	0.60~0.63
22~45	0.58~0.75	0.53~0.82
45~60	0.78~0.80	0.64~0.89

3. Calculation of Correction Factor

3.1. Calibration of Reaction Time Correction Factor

3.1.1. Determination of Correction Factor. According to the previous analysis, the main affecting factors of the reaction time come from the driver, vehicle, weather, and road condition, which can be considered four analytical indicators. This study uses a comprehensive weighted assessment method to calculate the various influencing factors based on the driver with normal driving technology and normal driving environment [25, 26]. The percentage system is used to evaluate and score the four analytical indicators for obtaining the state vector of each influencing factor:

$$\begin{aligned} F &= (F_1, F_2, F_3, F_4), \\ F_1 &= 0.6x_{11} + 0.25x_{12} + 0.15x_{13}, \\ F_2 &= 0.5x_{21} + 0.3x_{22} + 0.2x_{23}, \\ F_3 &= x_{31}, \\ F_4 &= 0.5x_{41} + 0.4x_{42} + 0.2x_{43}. \end{aligned} \tag{1}$$

x_{11}, x_{12}, and x_{13} indicate the scores of drivers' age, fatigue levels, and driving behavior styles, respectively. x_{21}, x_{22}, and x_{23} are the scores of the vehicle grade, service life ratio, and accident rate, respectively. x_{31} denotes the score of the weather condition, and the factor is multiplied by 0.8 if the driver is driving at night. x_{41}, x_{42}, and x_{43} indicate the scores of whether the road section is normal, the new and old quality of the road surface, and the road width (or the number of the single and two-way lanes), respectively.

If each indicator has a weighting factor, then the weight vector is

$$\omega = (\omega_1, \omega_2, \omega_3, \omega_4)^T, \tag{2}$$

where $\omega_j \geq 0\,(j = 1, 2, 3, 4)$ and $\sum_{j=1}^{4} \omega_j = 1$.

The comprehensive weighting method is used to construct a linear evaluation model for various indicators and reaction time:

$$y = (F, \omega) = \sum_{j=1}^{4} F_j \omega_j. \tag{3}$$

Based on the comprehensive evaluation value y of the vehicles' safe driving state under normal condition, we can obtain the correction factor k of driver's response time as $k = \sqrt{75/y}$.

The normal braking reaction time of the driver under normal driving condition is set to $t_{1,\mathrm{II}} = 1.25$ s, the minimum safety distance is set to $D = 2.5$ m, and the corrected t_r and D_r are

$$\begin{aligned} t_r &= k t_{1,\mathrm{II}} = 1.25k, \\ D_r &= k\,D = 2.5k. \end{aligned} \tag{4}$$

3.1.2. Determination of Weight Coefficient. The system analysis method is used to determine the weight coefficient of the analysis index $\omega_j\,(j = 1, 2, 3, 4)$, and the weight coefficients of the four indicators are compared in pair [27]. The result is recorded as matrix $A = A(a_{ik})$. The assignment criteria for a_{ik} are shown in Table 2, and $a_{ik}\,(i, k = 1, 2, 3, 4)$ indicates the ratio of the relative importance of the analysis indicators F_i and F_k about the evaluation target.

We have interviewed more than 100 drivers in the questionnaire form to collect potential important traffic factors. The final results from the questionnaire show that driver age span, driving experience, travelling type, and gender are considered as more important in comparison with other factors. From the survey results combined with Table 1, we can obtain

$$A = A(a_{ik}) = \begin{bmatrix} \omega_1/\omega_1 & \omega_1/\omega_2 & \omega_1/\omega_3 & \omega_1/\omega_4 \\ \omega_2/\omega_1 & \omega_2/\omega_2 & \omega_2/\omega_3 & \omega_2/\omega_4 \\ \omega_3/\omega_1 & \omega_3/\omega_2 & \omega_3/\omega_3 & \omega_3/\omega_4 \\ \omega_4/\omega_1 & \omega_4/\omega_2 & \omega_4/\omega_3 & \omega_4/\omega_4 \end{bmatrix} = \begin{bmatrix} 1 & 4 & 3 & 7 \\ 1/4 & 1 & 4 & 7 \\ 1/3 & 1/4 & 1 & 7 \\ 1/7 & 1/7 & 1/7 & 1 \end{bmatrix}. \tag{5}$$

The weight vector $\omega = (\omega_1, \omega_2, \omega_3, \omega_4)^T$ is used to left-multiply the matrix A. Then, the characteristic equation of the matrix A can be obtained as

$$\omega = \xi\omega, \tag{6}$$

where ξ is the eigenvalue and the calculated weight coefficients are $\omega_1 = 0.4969$, $\omega_2 = 0.2636$, $\omega_3 = 0.0797$, and $\omega_4 = 0.0396$.

3.2. Calculation of Road Surface Adhesion Coefficient.

Note that we can obtain the friction coefficient value with two different working logics, which are empirical-like methods and the nonlinear relevant models. Previous studies suggested that solutions obtained by empirical relevant models may not be very robust, which may further degrade traffic modeling accuracy [28–32]. It is noted that the relationship between the friction coefficient and the typical traffic relevant factors (i.e., road conditions, tire structural parameters, and vehicle speed) is a type of nonlinear function. Based on that we employ the artificial neural network for obtaining the optimal friction coefficient value.

The texture of tire is divided into three categories, namely, ordinary pattern, cross-country pattern, and mixed pattern, to establish the network structure. In this network structure, the input has three parameters: road condition, tire pressure, and vehicle speed; the output is the adhesion coefficients of each tire type. The BP neural network structure adopts a three-layer structure, that is, an input layer, two hidden layers, and an output layer. The input layer contains three layers of input. The first and second layers have four neurons and three neurons, respectively, and the

Table 2: Evaluation criteria of a_{ik}.

a_{ik}	Indicating
1	F_i is as important as F_k
3	F_i is slightly more important than F_k
5	F_i is evidently more important than F_k
7	F_i is considerably more important than F_k
9	F_i is extremely more important than F_k
2, 4, 6, 8	Corresponding to the intermediate situation of the two aforementioned adjacent judgments
Reciprocal	a_{ki} is a comparison judgment of $F_k$and F_i, $a_{ki} = 1/a_{ik}$

output layer has a single output, as shown in Figure 1. The training data is obtained from 120 experimental sample under 2 road surface (asphalt and cement concrete), different weather, and different driving speed.

The input layer uses the log-sig, tan-sig, and purelin functions as transfer functions:

$$Q^1(x) = \frac{1}{1+e^{-x}},$$
$$Q^2(x) = \frac{2}{(1+e^{-2x})} - 1, \quad (7)$$
$$Q^3(x) = x.$$

The relationship between input and output is

$$a^3 = Q^3\left\{\omega^3 Q^2\left[\omega^2 Q^1\left(\omega^1 I + d^1\right) + d^2\right] + d^3\right\}, \quad (8)$$

where $I_i \geq 0\,(i = 1, 2, 3)$ is an input parameter; ω^j and d^j denote the weight matrix and an offset value vector at $j\,(j = 1, 2, 3)$ layer. When $j = 3$, the layer represents an output layer; f^3 is an output parameter.

We have implemented experiments with varied tire pressures and vehicle speeds for obtaining the tire adhesion coefficient. More specifically, we have collected 108, 106, and 108 samples for the three typical tire patterns (i.e., ordinary, cross-country, and mixed patterns) and further test the tire adhesion coefficients. Typical training samples are shown in Table 3.

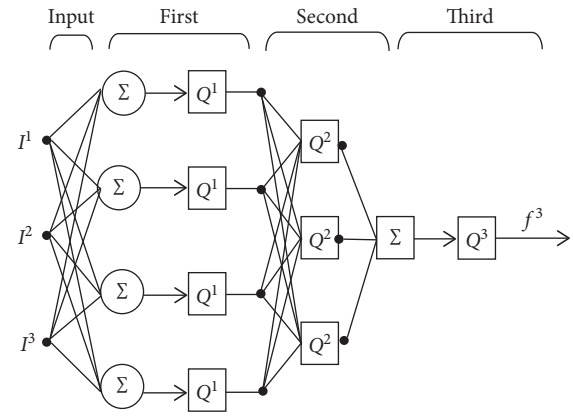

Figure 1: Neural network structure.

4. Methodology

4.1. Outline. For the purpose of readability, we firstly introduce our model flowchart in brief. We first analyze the vehicle breaking procedure, and the vehicle breaking distance (i.e., minimal safety distance) is estimated considering varied leading-vehicle states. Then, we explore speed correlations between two neighboring vehicles (leading and following vehicles) at different driving states. After that we establish an improved minimum safety distance model considering the factors of driver response time and road adhesion coefficient correction. Besides, we have collected data sources used in our study with the empirical and experimental manners.

4.2. Analysis of Vehicle Braking Process. During braking, the deceleration of vehicle changes with time, as shown in Figure 2 [1, 30]. Phase I is the reaction phase before performing, and Phase II is the coordination phase between the brake pedal and the vehicle. The time of the two phases is combined to obtain a value of 0.8–2.0 s. Phase III is the stage of deceleration growth and has a value of 0.1–0.2 s. Phase IV is a stage of stable uniform deceleration.

The reaction time of each stage is set to $t_{\mathrm{I,II}}$, t_{III}, and t_{IV}; the driving distances are $s_{\mathrm{I,II}}$, s_{III}, and s_{IV}; the initial speed of leading vehicle A and following vehicle B is v_1 and v_2, respectively; and the maximum deceleration is $a_{\max}$. According to the research in the literature [1], the calculation formula of the braking distance of the vehicle during a complete braking process is

$$s = v_1\left(t_{\mathrm{I,II}} + \frac{t_{\mathrm{III}}}{2}\right) + \frac{v_1^2}{2a_{\max}}. \quad (9)$$

4.3. Minimum Safe Distance Model. Vehicles A and B are set to drive in the same direction at speeds of v_{A} and v_{B}, respectively. The distance and speed difference of the two vehicles are S andv_0. The driving distance and acceleration of the two vehicles are S_{A}, S_{B}, a_{A}, and a_{B}, respectively. The actual driving situation can be divided into three types as follows.

4.3.1. Leading Vehicle Is at the Static State. When vehicle A is at the static state, that is, $v_{\mathrm{A}} = 0$ and $S_{\mathrm{A}} = 0$. Thus, when vehicle B brakes to stop, it should maintain the safe distance D of 2–5 m with vehicle A. Therefore, the initial safe distance between vehicles B and A should be

Table 3: Corresponding relationship between different tire patterns and adhesion coefficient under main influencing factors.

Tire pattern	No	Tire pressure (kPa)	Speed (km/h)	Road condition	Adhesion coefficient
Ordinary pattern	1	0.90	238	90	1.02
	2	0.90	238	75	1.13
	3	0.75	180	60	0.94
	4	0.75	180	45	0.92
	...	...	...	...	...
	108	0.10	112	60	0.16
Cross-country pattern	1	0.90	238	40	0.98
	2	0.90	198	40	1.01
	3	0.75	180	75	0.95
	4	0.75	160	75	0.82
	...	...	...	...	...
	106	0.10	238	90	0.14
Mixed pattern	1	0.90	238	40	1.02
	2	0.90	198	40	1.03
	3	0.75	180	75	0.92
	4	0.75	160	75	0.89
	...	...	...	...	...
	108	0.10	238	90	0.12

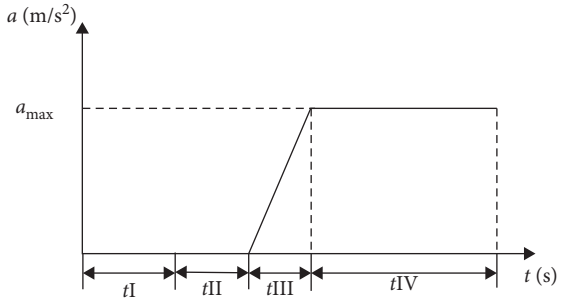

Figure 2: The changing process of deceleration.

$$S = v_B\left(t_{I,II} + \frac{t_{III}}{2}\right) + \frac{v_B^2}{2a_B} + D. \tag{10}$$

4.3.2. Leading Vehicle Is at the Uniform Driving State. When vehicle A is at the uniform driving state, there are two situations to be analyzed:

(a) $v_B > v_A$, the relative speed v_0 is large, and the vehicle following safety can be guaranteed only when vehicle B decelerates to $v_B = v_A$.

(b) $v_B > v_A$, the relative speed v_0 is small, and vehicle B is assumed to decelerate to $v_B = v_A$ at a certain time t_{III}' in the t_{III} interval. Accordingly, the vehicle following safety can be guaranteed at the same speed.

After calculating the driving distances of vehicles A and B, the initial safe distances between the two vehicles are obtained as

$$S = \begin{cases} v_0\left(t_{I,II} + \dfrac{t_{III}}{2}\right) + \dfrac{(v_B - v_A)^2}{2a_B} + D, & v_B > v_A, v_0 \text{ is large,} \\ v_0\left(t_{I,II} + t_{III}'\right) - \dfrac{a_B t_{III}'^2}{6} + D, & v_B > v_A, v_0 \text{ is small.} \end{cases} \tag{11}$$

4.3.3. Leading Vehicle Is at the Decelerating Driving State. When vehicle A is at the decelerating driving state, it can be further divided into three types:

(a) $v_B > v_A$, in this state, the vehicle B must brake to decelerate in time. Otherwise, there will be a rear-end collision accident. However, the vehicle B will apply brake after a certain reaction time when the driver finds that vehicle A is decelerating.

(b) $v_B = v_A$, under these circumstances, the vehicle B decelerates in order to reach the condition that two vehicles' speed is equal. At meantime, in order to ensure the safety of car-following, the distance between two adjacent vehicles should be equal to the minimum safety distance.

(c) $v_B < v_A$, in this state, the car-following is safe at beginning, but it will change when the vehicle A drives at a constant deceleration and the vehicle B drives at a constant speed. When the vehicle A decelerates to reach the condition $v_A \le v_B$, this state will change to the first two situations. For convenience of calculation, the deceleration of vehicle A is assumed to reach the maximum when $v_A = v_B$. Then, the required deceleration time can be calculated as follows: $t_m = t_{III} + (v_A - a_A t_{III}/2 - v_B)/a_A$. Thereafter, vehicle B must decelerate to ensure the safe following of the two vehicles. After calculating the driving distances of vehicles A and B, the initial safe distances between the two vehicles in three cases are obtained as

$$S = \begin{cases} v_B t_{I,II} + \dfrac{(v_B - v_A)t_{III}}{2} + \dfrac{v_B^2}{2a_B} - \dfrac{v_A^2}{2a_A} + D, & v_B > v_A, \\ v_B t_{I,II} + \dfrac{v_B^2}{2a_B} - \dfrac{v_A^2}{2a_A} + D, & v_B = v_A, \\ v_B\left(t_{I,II} + t_{III}\right) - \dfrac{2v_B^2 - 2v_B v_A + v_A^2 + v_A^2}{2a_A} + \dfrac{v_B^2}{2a_B} - \dfrac{v_A t_{III}}{2} + D, & v_B < v_A. \end{cases} \tag{12}$$

4.4. Correction of Minimum Safe Distance Model. In the process of vehicle braking, the brake deceleration is limited by the adhesion coefficient of road surface, that is,

$$a \le \mu g, \tag{13}$$

where μ is the adhesion coefficient and g is the gravitational acceleration. When the model is corrected, the constraint is taken as an equal sign, and the maximum deceleration of vehicles A and B in the model is replaced by the adhesion coefficient.

Correction of the model: according to the analysis results of Section 3.1.1, the response time is $t_r = kt_{I,II} = 1.25k$ and the minimum safety distance is $D_r = k\,D = 2.5k$, where $k = \sqrt{75/y}$. Take the ordinary tires, for example, the calculated value of the output parameter is $a^3 = 0.892$ under the combination conditions of dry asphalt pavement, the tire pressure of 238 kPa, and the driving speed of 40 km/h. Therefore, the maximum deceleration is $a = \mu g = 0.892g$. After that the two parameters are integrated with the traditional minimum safety distance model.

4.4.1. Leading Vehicle Is at the Static State. The corrected model is

$$S = v_B\left(1.25k + \frac{t_{III}}{2}\right) + \frac{v_B^2}{2\mu_B g} + 2.5k. \tag{14}$$

4.4.2. Leading Vehicle Is at the Uniform Driving State. The corrected model is

$$S = \begin{cases} v_0\left(1.25k + \dfrac{t_{III}}{2}\right) + \dfrac{(v_B - v_A)^2}{2\mu_B g} + 2.5k, & v_B > v_A, v_0 \text{ is large}, \\ v_0\left(1.25k + t_{III}'\right) - \dfrac{\mu_B g t_{III}'^2}{6} + 2.5k, & v_B > v_A, v_0 \text{ is small}. \end{cases} \tag{15}$$

4.4.3. Leading Vehicle Is at the Decelerating Driving State. The corrected model is

$$S = \begin{cases} 1.25kv_B + \dfrac{(v_B - v_A)t_{III}}{2} + \dfrac{v_B^2}{2\mu_B g} - \dfrac{v_A^2}{2\mu_A g} + 2.5k, & v_B > v_A, \\ 1.25kv_B + \dfrac{v_B^2}{2\mu_B g} - \dfrac{v_A^2}{2\mu_A g} + 2.5k, & v_B = v_A, \\ v_B\left(1.25k + t_{III}\right) - \dfrac{2v_B^2 - 2v_B v_A + v_A^2}{2\mu_A g} + \dfrac{v_B^2}{2\mu_B g} - \dfrac{v_A t_{III}}{2} + 2.5k, & v_B < v_A. \end{cases} \tag{16}$$

5. Numerical Simulation and Analysis

5.1. Overview. We analyzed the main factors (i.e., vehicle condition, road status, weather condition, type speed, etc.) which influence the minimal vehicle safety distance. We have proposed an improved vehicle rear-end collision model to analyze such influence. More specifically, we firstly employed the response time correction and road adhesion coefficient parameters to quantify typical factors' influence (e.g., vehicle condition, road status, weather condition, and type speed). Then, the integrated weighting model and BP neural network were introduced to determine the optimal values for the two parameters for the improved minimal safety distance model. We have collected both the questionnaires and empirical data to obtain the weighting matrices and empirical tire patterns, which serves as the inputs for the integrated weighting model and BP neural network, respectively. Based on that we have further analyzed the relationships between the correlation between varied factors and minimal safety distance at five hypotheses. The experimental design overview is shown in Figure 3.

5.2. Parameter Setting. Based on experimental tests and existing research literature, this study considers that the reaction time is $t_{\mathrm{III}} = 0.18\,\mathrm{s}$ and $t'_{\mathrm{III}} = 0.12\,\mathrm{s}$ and the gravitational acceleration is a constant ($g = 9.8\,\mathrm{m/s^2}$). In Section 3.1, the value of each weight coefficient has been calculated (i.e.,$w_1 = 0.497$, $w_2 = 0.264$, $w_3 = 0.080$, and $w_4 = 0.040$, where $w_j\,(j = 1, 2, 3, 4)$ represents the characteristics of the driver, the weighting coefficient of the vehicle, and weather and road conditions.).

In order to carry out single factor impact analysis, five comparisons are assumed (as shown in Table 4). The condition of "Hypothesis 1" is the standard state (as a comparative object), and other hypothesis is set by changing a certain factor based on the case of "Hypothesis 1" for comparing the analysis results (e.g., when analyzing the impact of weather on driving safety, set the condition of "Hypothesis 4" based on the case of "Hypothesis 1"). The variable y denotes comprehensive evaluation value, and the variable k denotes correction factor. For each hypothesis, the value of variable y and k can be calculated.

Ordinal note: *Driver*, set two categories, very experienced and generally experienced. The main difference of two kinds of drivers is the reaction time and the estimation of car-following distance. *Vehicle*, set two categories, and the first category is the high-end and well-maintained vehicle and the other is the medium-end and generally maintained vehicle. *Weather*, set two categories, sunny and rainy. In sunny weather, the drivers have good driving sight and can more accurately judge the distance and relative speed from the front car. In rainy weather, the opposite occurs. *Road*, set two categories, new and old. The new road denotes that the road is newly built, and the pavement condition is better. The old road denotes that the road has been built for many years, and the pavement condition is worse.

5.3. Simulation Analysis

5.3.1. Leading Vehicle Is at the Static State. Figure 4 shows the results when the speed of following vehicle B changes from 40 km/h to 60 km/h. Under the five simulation situations, the minimum safe distance increases with the increase of speed of vehicle B (the value of the safe distance is between 147 m and 157 m). The x-axis represents the speed of vehicle B, and the y-axis represents the required minimum safe following distance in Figure 4. It appears that the minimum safe distance in condition of "Hypothesis 1" is the smallest and is the biggest in condition of "Hypothesis 3."

On the basis of "Hypothesis 1," when the speed of vehicle B is constant, changing any of the four factors changes the minimum safety distance at different degrees. By contrast, the greatest change in the minimum safe distance is in condition of "Hypothesis 3," that is to say the vehicle situation has the greatest impact on the minimum safe distance, whereas the smallest change in minimum safety distance is in condition of "Hypothesis 5," that is to say the road condition has the least impact.

5.3.2. Leading Vehicle Is at the Uniform Driving State. When vehicle A is at the uniform driving state and its speed is 40 km/h, the results under different situations are as follows:

(a) $v_{\mathrm{B}} > v_{\mathrm{A}}$, the relative speed v_0 is large.

Figure 5 shows the simulation results when the speed of vehicle B changes from 60 km/h to 65 km/h and the relative speed changes to 20–25 km/h. The x-axis represents the relative speed of two adjacent vehicles and the y-axis represents the required minimum safe following distance in Figure 5. The value of the minimum safe distance is between 51 m and 61 m.

(b) $v_{\mathrm{B}} > v_{\mathrm{A}}$, the relative speed v_0 is small.

Figure 6 shows the simulation results when the speed of vehicle B changes from 45 km/h to 50 km/h and the relative speed changes to 5–10 km/h. The representation of x-axis and y-axis in Figure 6 is the same with that of Figure 5. The value of the minimum safe distance is between 8.5 m and 12.5 m.

Figures 5 and 6 show that the required safe following distance is positive proportional to the relative speed of two adjacent vehicles. When the relative speed is large, the required safe following distance under the three other hypotheses changes more than that under "Hypothesis 1." It appears that the minimum safe distance in condition of "Hypothesis 1" is the smallest and is the biggest in condition of "Hypothesis 3."

Similarly, on the basis of "Hypothesis 1," when the speed of vehicle B is constant, changing any of the three remaining factors changes the minimum safety distance at different degrees. By contrast, the greatest change in the minimum safe distance is in condition of "Hypothesis 3," that is to say the vehicle situation has the greatest impact on the minimum safe distance, whereas the smallest change in

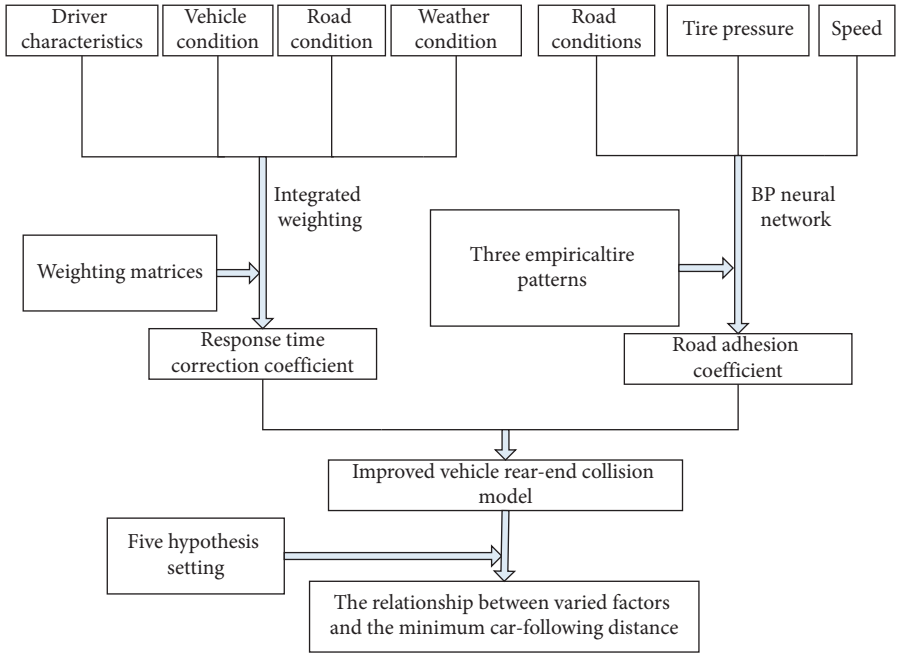

Figure 3: Schematic view of the experimental design.

Table 4: Simulation condition setting.

	Driver	Vehicle	Weather	Road	y	k
Hypothesis 1	Very experienced	High-end car, well maintained	Sunny	New	76.838	0.988
Hypothesis 2	Generally experienced	High-end car, well maintained	Sunny	New	70.751	1.030
Hypothesis 3	Very experienced	Medium-end car, generally maintained	Sunny	New	68.930	1.043
Hypothesis 4	Very experienced	High-end car, well maintained	Rainy	New	74.049	1.006
Hypothesis 5	Very experienced	High-end car, well maintained	Sunny	Old	76.046	0.993

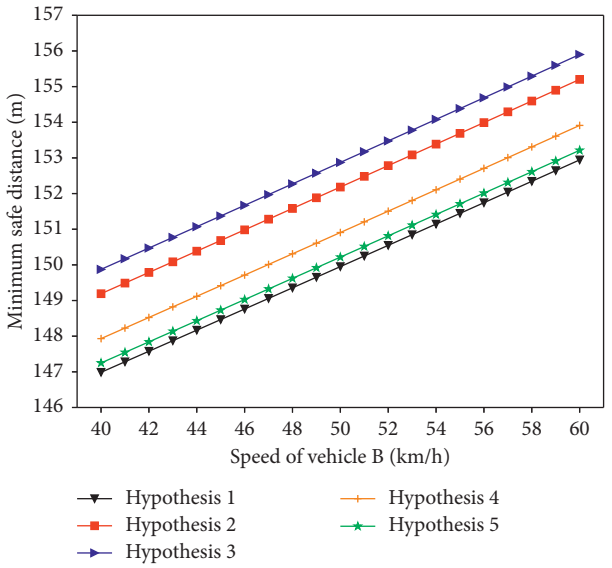

Figure 4: Simulation results at static state of vehicle A.

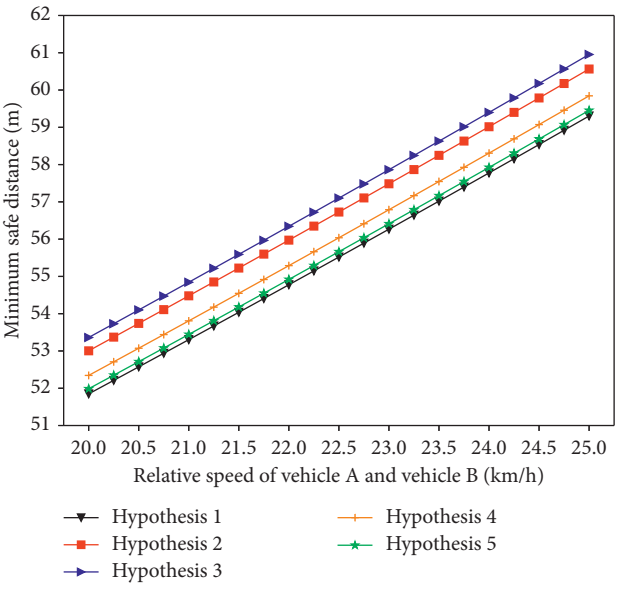

Figure 5: Simulation results at large relative speed.

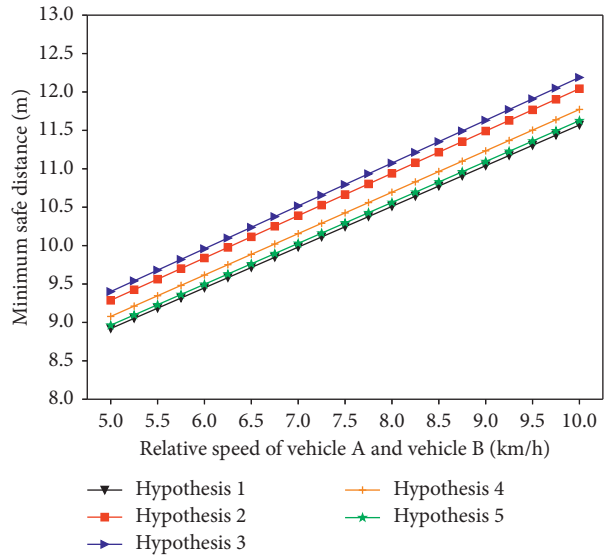

Figure 6: Simulation results at small relative speed.

minimum safety distance is in condition of "Hypothesis 5," that is to say the road condition has the least impact.

5.3.3. Leading Vehicle Is at the Decelerating Driving State. There are three situations:

(a) $v_B > v_A$, Figure 7 shows the simulation results when the speed of vehicle A changes from 40 km/h to 50 km/h and that of vehicle B changes to 60–70 km/h. The x-axis represents the speed of vehicle B, the y-axis represents the speed of vehicle A, and the z-axis represents the required minimum safe following distance in Figure 7. The value of the minimum safe distance is between 192 m and 204 m.

(b) $v_B = v_A$, Figure 8 shows the simulation results when the speed of vehicle A changes from 40 km/h to 50 km/h and the speed of the two vehicles is equal. The representation of x-axis, y-axis, and z-axis in Figure 8 is the same as that of Figure 7. The value of the minimum safe distance is between 51 m and 58 m.

(c) $v_B < v_A$, Figure 9 shows the simulation results when the speed of vehicle A changes from 60 km/h to 70 km/h and the speed of vehicle B changes to 40–50 km/h. The representation of x-axis, y-axis, and z-axis in Figure 9 is the same as that of Figure 7. The value of the minimum safe distance is between 30 m and 37 m.

Comparison of Figures 7–9 indicates that when vehicle A is at the uniform decelerating state, the required minimum safety distance is the largest when the speed of vehicle B is large than that of vehicle A, and its value is more than 190 m and is the smallest when the speed of vehicle A is large than that of vehicle B, and its value is below 35 m. The required minimum safe distance is between the abovementioned two

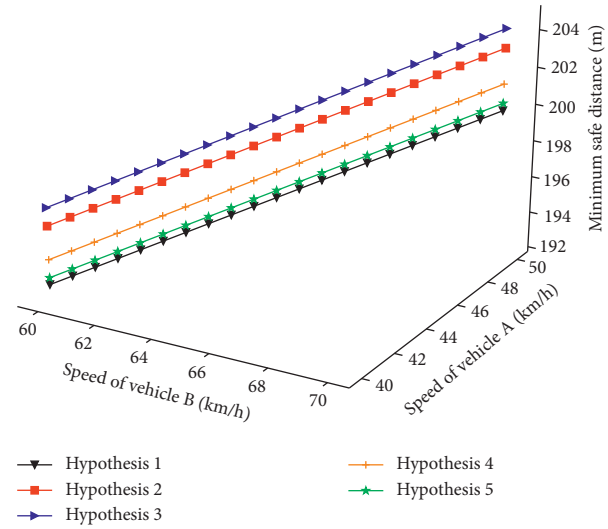

Figure 7: Simulation results of rear vehicle at high speed.

values when the speed of vehicle A is equal to that of vehicle B, and its value is about 50 m. The simulation results coincide with the actual driving situation. From the three figures, it can be seen that the minimum safe distance in condition of "Hypothesis 1" is the smallest and is the biggest in condition of "Hypothesis 3."

Similarly, on the basis of Hypothesis 1, when the speed of vehicle B is constant, changing any of the three remaining factors changes the minimum safety distance at different degrees. By contrast, the greatest change in the minimum safe distance is in condition of "Hypothesis 3," that is to say the vehicle situation has the greatest impact on the minimum safe distance, whereas the smallest change in minimum safety distance is in condition of "Hypothesis 5," that is to say the road condition has the least impact.

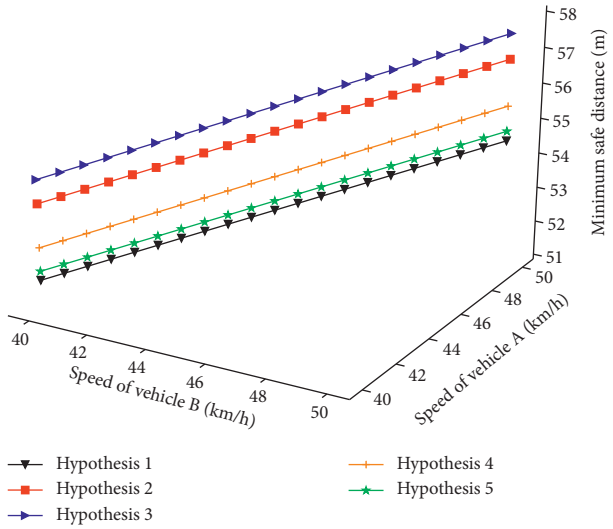

Figure 8: Simulation results of two vehicles at constant speed.

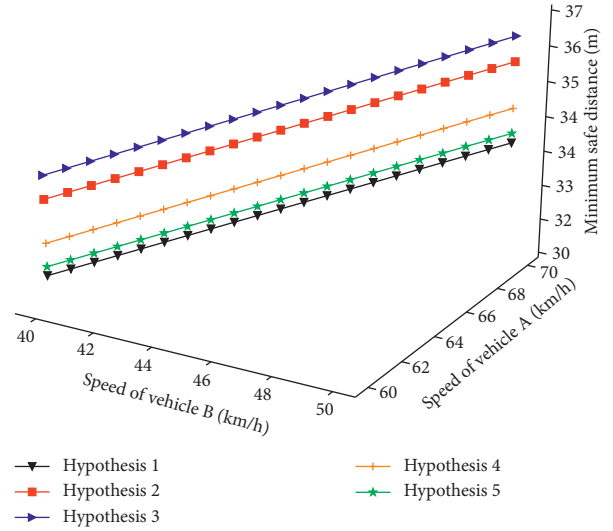

Figure 9: Simulation results of front vehicle at high speed.

6. Conclusions

Minimal car-following distance is very crucial for ensuring roadway traffic safety. By analyzing driving interference factors in both qualitative and quantitative manner, we estimated the minimal traffic safety distance between neighboring vehicles. More specifically, we employed response time and road adhesion coefficient for the purpose of quantifying various factors impact on the minimal traffic safety distance, which were integrated with the traditional minimum safety distance model. We conducted a series of experiment to verify our model performance in the typical car-following state, with the vehicle-ahead in different driving conditions (i.e., static state, uniform driving state, and decelerating driving state). The specific conclusions were shown as follows:

(1) By considering typical vehicle-ahead states, we analyzed the relationship between the vehicle speed and the minimum safety distance. More specifically, positive correlation was found between the minimal safety distance and the relative speed of the ahead and behind neighboring vehicles. Larger relative vehicle speed requires larger minimum safety distance, and vice versa.

(2) We have tested the minimum safety distance distribution considering impact from driver, vehicle, road, and environment. It is noted that the minimum safety distance is more sensitive to the vehicle situation and less affected by the road condition. In that manner, traffic regulations are suggested to pay more attention to the vehicle state (e.g., tire peruse and engine healthy state) for the purpose of ensuring roadway safety.

(3) The findings of our study can benefit autonomous driving vehicle safety and provide theoretical support for enhancing roadway traffic efficiency and safety.

Data Availability

All data used to support the findings of this study are included within the article.

Conflicts of Interest

The authors declare no conflicts of interest.

Authors' Contributions

Conceptualization was carried out by Qiang Luo and Xinqiang Chen; data curation was carried out by Shubo Wu; formal analysis was performed by Qiang Luo; funding acquisition was done by Xiaodong Zang; investigation was carried out by Shubo Wu; methodology was drawn by Qiang Luo, Xiaodong Zang, and Xinqiang Chen; project administration was looked after by Jie Yuan; resources was looked after by Junheng Yang; software was taken care by Xiaodong Zang and Jie Yuan; supervision was conducted by Junheng Yang; validation was performed by Junheng Yang and Shubo Wu; visualization was performed by Shubo Wu; writing the original draft was carried out by Qiang Luo; writing the review and editing was carried out by Jie Yuan and Xinqiang Chen.

Acknowledgments

This work was supported by the National Natural Science Foundation of China (51908151, 51867009, 51579143, and 51709167), Natural Science Foundation of Guangdong Province, China (2019A1515010701 and 2017A030313293), Foundation Plan for Distinguished Young Scholars in Jiangxi Province, China (20162BCB23045), Applied and Cultivation Program of Science and Technology Department of Jiangxi Province, China (20181BBE58010), Guangzhou University Research Project (YG2020004), and Shanghai Committee of Science and Technology China (18040501700, 18295801100, and 17595810300).

References

[1] L. H. Xu, Q. Luo, J. W. Wu et al., "Study of car-following model based on minimum safety distance," *Journal of Highway and Transportation Research and Development*, vol. 27, no. 10, pp. 95–100, 2010.

[2] D. H. Wang and S. Jing, "Review and outlook of modeling of car-following behavior," *China Journal of Highway and Transport*, vol. 25, no. 1, pp. 115–127, 2012.

[3] H. Hao, W. Ma, and H. Xu, "A fuzzy logic-based multi-agent car-following model," *Transportation Research Part C: Emerging Technologies*, vol. 69, pp. 477–496, 2016.

[4] B.-G. Cao, "A new car-following model considering driver's sensory memory," *Physica A: Statistical Mechanics and Its Applications*, vol. 427, pp. 218–225, 2015.

[5] J. S. Kong, F. Guo, and X. P. Wang, "A vehicle rear-end anti-collision method based on safety distance model," *Microcomputer Information*, vol. 32, pp. 251-252, 2008.

[6] N. H. Jiang and J. G. Yu, "Study on rear-end avoidance model of highway based on neural network," *Forest Engineering*, vol. 26, no. 5, pp. 60–62, 2010.

[7] S. Jing and D. H. Wang, "Car-following model and simulation considering front traffic situation," *Journal of Beijing University of Technology*, vol. 38, no. 8, pp. 1236–1241, 2012.

[8] D. H. Xia, "Research of automobile anti-collision safety distance model based on characteristics of the driver," Master's thesis, Liaoning University of Technology, Jinzhou, China, 2016.

[9] G. H. Peng and D. H. Sun, "A dynamical model of car-following with the consideration of the multiple information of preceding cars," *Physics Letters A*, vol. 374, no. 15-16, pp. 1694–1698, 2010.

[10] R. E. Wilson and J. A. Ward, "Car-following models: fifty years of linear stability analysis-a mathematical perspective," *Transportation Planning and Technology*, vol. 34, no. 1, pp. 3–18, 2011.

[11] H.-S. Tan and J. Huang, "DGPS-based vehicle-to-vehicle cooperative collision warning: engineering feasibility viewpoints," *IEEE Transactions on Intelligent Transportation Systems*, vol. 7, no. 4, pp. 415–428, 2006.

[12] X. Huang, J. Sun, and J. Sun, "A car-following model considering asymmetric driving behavior based on long short-term memory neural networks," *Transportation Research Part C: Emerging Technologies*, vol. 95, pp. 346–362, 2018.

[13] X. Na and D. J. Cole, "Game-theoretic modeling of the steering interaction between a human driver and a vehicle collision avoidance controller," *IEEE Transactions on Human-Machine Systems*, vol. 45, pp. 5–38, 2014.

[14] K. Fadhloun and H. Rakha, "A novel vehicle dynamics and human behavior car-following model: model development and preliminary testing," *International Journal of Transportation Science and Technology*, vol. 9, no. 1, pp. 14–28, 2020.

[15] J. Tang, F. Liu, W. Zhang, R. Ke, and Y. Zou, "Lane-changes prediction based on adaptive fuzzy neural network," *Expert Systems with Applications*, vol. 91, pp. 452–463, 2018.

[16] Y. Zou, X. Ye, K. Henrickson, J. Tang, and Y. Wang, "Jointly analyzing freeway traffic incident clearance and response time using a copula-based approach," *Transportation Research Part C: Emerging Technologies*, vol. 86, pp. 171–182, 2018.

[17] X. Ma, S. Sun, X. C. Liu, C. Ding, Z. Chen, and Y. Wang, "A time-varying parameters vector auto-regression model to disentangle the time varying effects between drivers' responses and tolling on high occupancy toll facilities," *Transportation Research Part C: Emerging Technologies*, vol. 88, pp. 208–226, 2018.

[18] N. L. Brocn and D. P. Chiang, "Braking response times for 100 drivers in the avoidance of an unexpected obstacle as measured in a driving simulator," *Proceedings of the Human Factors and Ergonomics Society 4th Annual Meeting*, vol. 40, no. 18, pp. 900–904, 1996.

[19] Q. Luo, X. Chen, J. Yuan, X. Zang, J. Yang, and J. Chen, "Study and simulation analysis of vehicle rear-end collision model considering driver types," *Journal of Advanced Transportation*, vol. 2020, Article ID 7878656, 11 pages, 2020.

[20] Y. G. Zhang, S. G. Hu, and X. Y. Kuang, "Car-following model based on man-vehicle-road-environment," *Highway*, vol. 60, no. 3, pp. 139–145, 2015.

[21] J. X. Xu and J. S. Wu, "Harsh environment influence on drivers' response time," *Transport Standardization*, vol. 210, pp. 103–106, 2009.

[22] S. L. Li and Y. L. Pei, "Analysis of influencing factors of pavement adhesion performance and improvement measures," *Highway*, vol. 11, pp. 21–25, 2007.

[23] Y. G. Huang, L. H. Xu, and X. Y. Kuang, "Urban road traffic state identification based on fuzzy C-mean clustering," *Journal of Chongqing Jiaotong University (Natural Science)*, vol. 34, no. 2, pp. 101–106, 2015.

[24] X. Chen, S. Wang, C. Shi, H. Wu, J. Zhao, and J. Fu, "Robust ship tracking via multi-view learning and sparse representation," *Journal of Navigation*, vol. 72, no. 1, pp. 176–192, 2019.

[25] Y. Zou, J. E. Ash, B.-J. Park, D. Lord, and L. Wu, "Empirical Bayes estimates of finite mixture of negative binomial regression models and its application to highway safety," *Journal of Applied Statistics*, vol. 45, no. 9, pp. 1652–1669, 2018.

[26] S. Yu, R. Fu, Y. Guo, Q. Xin, and Z. Shi, "Consensus and optimal speed advisory model for mixed traffic at an isolated signalized intersection," *Physica A: Statistical Mechanics and Its Applications*, vol. 531, p. 121789, 2019.

[27] Q. Luo, J. Yuan, X. Q. Chen et al., "Analyzing start-up time headway distribution characteristics at signalized intersections," *Physica A: Statistical Mechanics and Its Applications*, vol. 535, pp. 1–10, 2019.

[28] S. L. Li, Y. L. Pei, and T. F. Lei, "Calculation model for adhesion coefficient based on neural networks system," *Journal of Northeast Forestry University*, vol. 36, no. 2, pp. 56-57, 2008.

[29] X. Chen, Y. Yang, S. Wang et al., "Ship type recognition via a coarse-to-fine cascaded convolution neural network," *Journal of Navigation*, vol. 2020, pp. 1–20, 2020.

[30] X. Q. Chen, L. Qi, Y. S. Yang et al., "Video-based detection infrastructure enhancement for automated ship recognition and behavior analysis," *Journal of Advanced Transportation*, vol. 202012 pages, 2020.

[31] X. Chen, X. Xu, Y. Yang, H. Wu, J. Tang, and J. Zhao, "Augmented ship tracking under occlusion conditions from maritime surveillance videos," *IEEE Access*, vol. 8, pp. 42884–42897, 2020.

[32] T. Q. Tang, J. G. Li, H. J. Huang, and X. B. Yang, "A car-following model with real-time road conditions and numerical tests," *Measurement*, vol. 48, pp. 63–76, 2014.